Springback in High Strength Anisotropic Steel

Oladipo Onipede Jr. – Assistant Professor
Carlos J. Gomes – Graduate Student
Mechanical Engineering Department
University of Pittsburgh
Benedum Engineering Hall
3700 O'Hara Street, office 648
Pittsburgh, PA 15261, USA.
onipede@pitt.edu
(412) 624-9606
(412) 624-4846 *fax*

Keywords:
Springback, High Strength Steel, Anisotropy, Non-linear Finite Element Analysis, Draw Forming.

ABSTRACT

This paper presents the finite element analysis and results of springback in a U-shape cross section made of high strength anisotropic steel. The results are compared with those obtained from two isotropic materials that have the same yield stresses as those of the principal directions of the anisotropic steel sheet. The principal directions are the directions of the sheet that have the largest and smallest yield stresses respectively. The results show the discrepancy between springback predicted by the isotropic and anisotropic materials, but also the variability of springback with respect to the angle of orientation of the anisotropic steel sheet. This may help address the question of when it is appropriate to use isotropic material properties for anisotropic materials when it comes to predicting springback.

INTRODUCTION

New high strength steels recently developed can have a significant impact in the automotive industry, where they can provide higher strength to weight ratios for structural parts. One of the main obstacles in introducing these steels into the industry is their unknown and unfamiliar behavior during the metal forming of parts. High strength steels by definition have a higher material yield stress (Dieter, 1986) and so will require higher forces to form parts and these parts will have a larger elastic recovery after forming. The study of this elastic recovery or Springback (SB) phenomenon is a very important issue that will influence and complicate the design of dies for specific parts. These high strength steels also tend to show a more significant level of anisotropy in their elastic properties and yield stresses. These anisotropic effects can cause twisting of parts during and after forming, which can further complicate the design of dies for forming. All these effects can significantly increase the cost and time necessary for the design phase of new or existing parts.

The SB is a consequence of the unbalanced stresses through the thickness of the section undergoing bending. Experimental studies (Stein, 1998) have shown a dependence on material behavior, thickness of the shell, level of plastic deformation, shape of the die, friction, stamping process, etc. On the other hand, computational studies and simulation of SB shows the sensitivity of the technique to different mathematical and computational parameters such as, number of integration points through the thickness, contact parameters, simulation speed, hourglass control, number and distribution of elements, etc (Shi, 1998 & 1999; Hu, 1999).

The results presented here are from the study of springback behavior in high strength anisotropic steels using the finite element technique. A **U** shaped cross-sections was analyzed and the forming-springback process is performed in a sequential explicit to implicit simulation

APPROACH

The **U** shaped cross-sections presented in NUMISHEET'93 (see Figure 1) was selected for this study, because it is a benchmark problem for isotropic springback analysis. There is also a specify standard to measure springback for this section (see Figure 2 for details). Since the shape is symmetric, only half of the model was employed, using the appropriate boundary conditions. The simulation was divided in two stages. The first stage of the simulation consist of a deep-drawing forming process; this step was performed explicitly with the finite element based package LS-DYNA version 950, which provides stability and low computational costs. The second stage of the simulation, the springback, which is based on the results from the unbalanced stresses and geometry of the last forming step, is performed implicitly with ANSYS 5.6. The details of these steps are explained in the following sections.

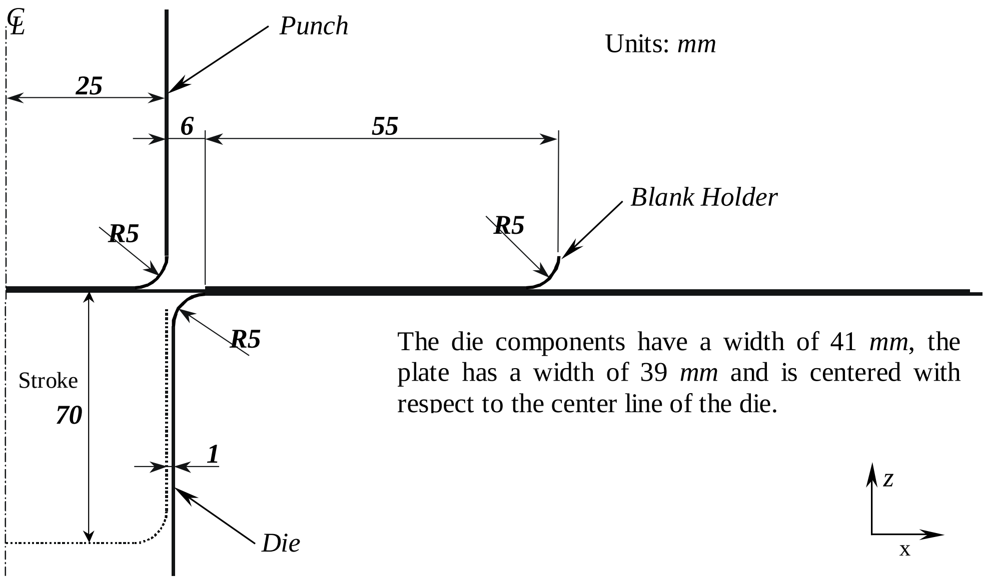

Figure 1. Scheme of NUMISHEET'93 benchmark.

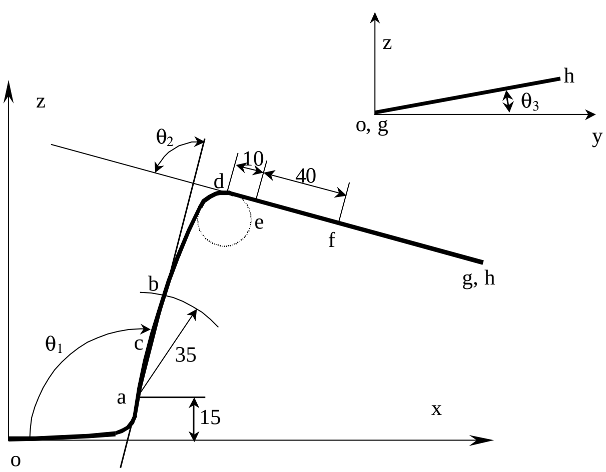

<u>Springback</u>
θ_1: Angle between ox and ab.
θ_2: Angle between ab and ef.

<u>Twister</u>
θ_3: Angle between oy and gh.

<u>Curvature</u>
ρ: Defined by the radius of a circle through a, b and c.

<u>Points</u>
a: 15 mm from ox.
b: 35 mm from point a.
c: Middle point of the straight line ab.
d: End of the Die's curvature.
e: 10 mm from d.
f: 40 mm from e.
g: front corner of the plate.
h: back corner of the plate.

Figure 2. Measuring method for springback and twister.

Draw forming

All the components of the die were simulated as rigid bodies. Therefore, only the surfaces of the die in contact with the blank were included in the model (see Figures 1 and 3). However, for the contact algorithm/mechanism an elastic material behavior and a thickness of 0.5*mm* were employed for these rigid components. The contact algorithm uses the elastic modulus and the thickness of the elements in contact in order to compute the penalty spring constant.

The elastic constants used are presented in Table 1. Five elements were used across the width and 16 elements were used in the tangent direction around the bends. The ratio of size change of the rigid element was controlled, in order to avoid abrupt changes in the penalty spring constant when the elements of the blank pass from one element to another.

Table 1. Material properties of the Die's component.

Property	Magnitude
Young's Modulus	207 Gpa
Poisson's ratio	0.223
Density	6830 $^{kg}/_{m}3$

The dimensions of the blank were 300x39x0.78 *mm*. 768 Hughes-Liu four nodes shell elements, with 128 along the length and 6 across the width (see Figure 3) were used. A shear factor of $^{5}/_{6}$ and a total of 5 integration points through the thickness were used in order to catch the variation of the stresses and strains through the thickness. The hourglass control based on Belytschko and Tsay viscous formulation was selected in order to avoid problems with single point gaussian integration. A coefficient of 0.1 was selected for in-plane, bending and warping hourglass.

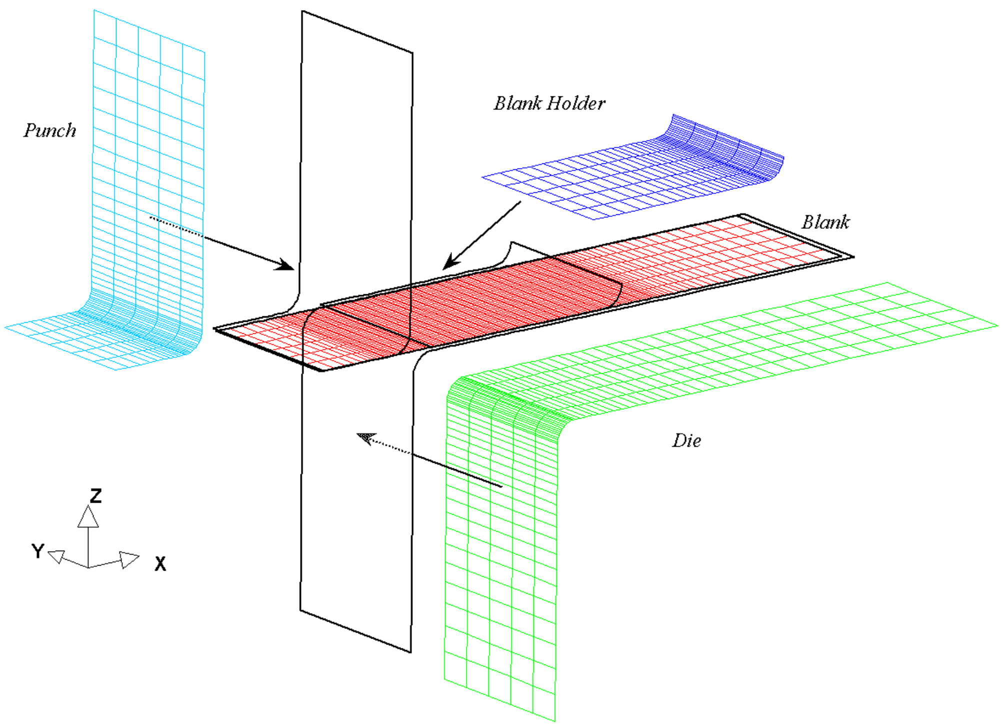

Figure 3. Finite element model.

The LS-DYNA material model 36 (Barlat's 3-parameter plasticity) was chosen because it can accommodate in-plane anisotropic yield behavior. This model combines isotropic elastic behavior with anisotropic plastic potential developed by Barlat and Lian (Barlat, 1989). This model also includes an isotropic linear strain-hardening rule, which is satisfactory since there are not significant plastic-strain reversals in the model. Tables 2 presents the elastic and plastic parameters and Figure 4 shows the variation of the yield stress to the angle with respect to the roller direction.

Table 2. Material parameters for the blank.

Parameter	Magnitude
Young's modulus	207 GPa.
Yield Stress (roller direction)	392 MPa.
Tangent modulus	1.63 MPa.
Poisson's ratio	0.223
Density	6830 $^{kg}/_{m^3}$.
Lankford parameter at 0^0	0.724
Lankford parameter at 45^0	0.903
Lankford parameter at 90^0	1.107
Barlat exponential parameter (m)	2.0

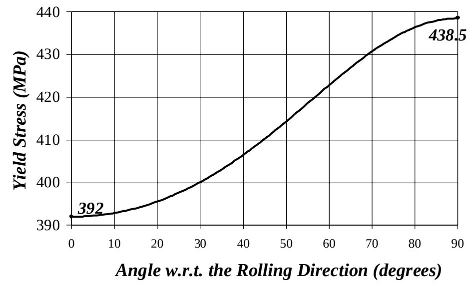

Figure 4. Yield stress of the blank to the angle w.r.t. the rolling direction.

Draw forming boundary and initial conditions

Table 3 presents the boundary conditions applied to the blank and die components during the draw-forming model. Figure 5 presents the punch speed profile as well as the blank holder force profile. The process finished in 52 *ms* and the blank was drawn 70 *mm* into the die's cavity.

Table 3. Boundary conditions applied to the blank and die components.

Component	Disp.			Rotation		
	x	*y*	*z*	θ_x	θ_y	θ_z
Punch	✓	✓	✓	✓	✓	✗
Die	✓	✓	✓	✓	✓	✓
Blank Holder	✓	✓	✓	✓	✓	✗
Blank's s.l.	✓	✗	✗	✗	✓	✓
Middle node at s.l.	✓	✓	✗	✗	✓	✓

Where:
✓ - Constrained.
✗ - Free.
s.l.: symmetric line

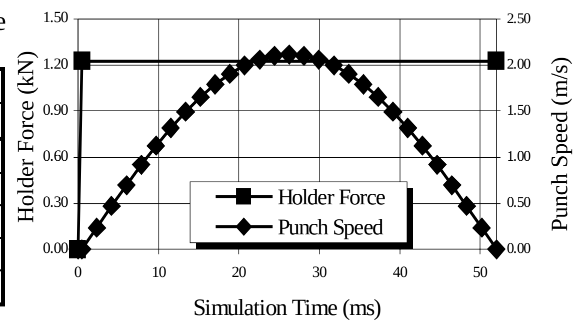

Figure 5. Variation of blank holder force and punch velocity with time.

Springback Analysis

The springback simulation is performed implicitly using the full Newton-Raphson method. It uses the results from the unbalanced stresses and geometry of the last forming step. For the springback analysis, the die components were removed and an isotropic linear elastic material model was used. The elastic properties from the forming model were kept.

Springback boundary conditions

The displacements of the symmetric line in the *z* direction were constrained in addition to the other boundary conditions from the forming analysis. This was done in order to prevent rigid body motions.

DISCUSSION OF RESULTS

The variation of the parameters θ_1, θ_2 and ρ (see Figure 2 for details) with respect to the material (blank) orientation angle are presented in Figure 6, 7 and 8, respectively. The figures also include these parameters for two hypothetic isotropic materials, which have the same yield stress as the extremes of the anisotropic material. These yield stresses are 392 MPa in the rolling direction and 438 MPa in the transversal direction. Figures 9 and 10 show two views of the springback.

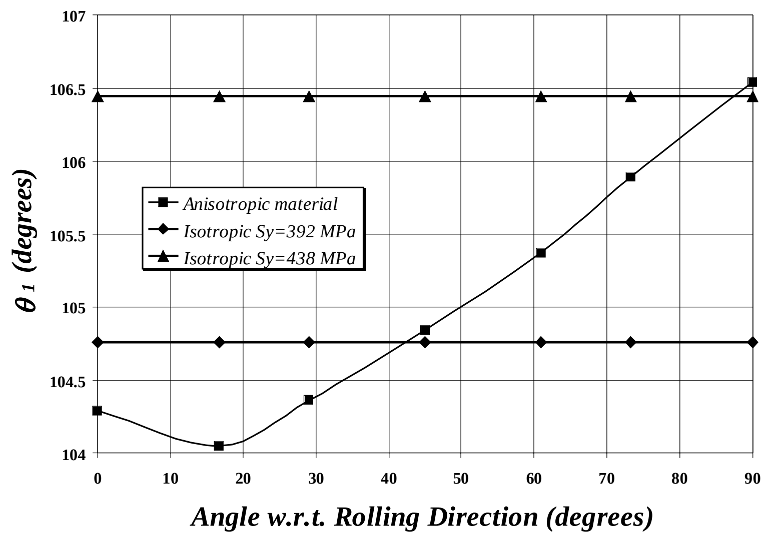

Figure 6. Variation of θ_1 to the angle w.r.t. the rolling direction.

Figure 6 shows that θ_1 increase with the yield stress for anisotropic material. It also shows that the springback of this bended section is affected by the yield stress in the transversal direction. The effect of a smaller transversal (with respect to the longitudinal) yield stress is to increase the springback and, vice versa for a bigger transversal yield stress. Another observation from Figure 6 is the discrepancy between the SB predicted by the isotropic yield criteria and the anisotropic one. The maximum amount of springback was found at the transversal direction.

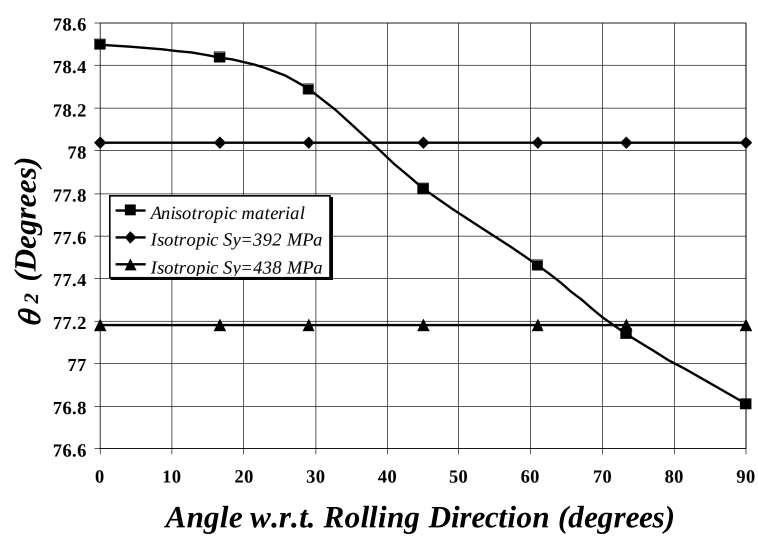

Figure 7. Variation of θ_2 to the angle w.r.t. the rolling direction.

Figure 7 shows that the SB increases with the yield stress (in this case θ_2=90^o means no SB) and the discrepancy between the predicted by isotropic material yield stress with respect to that predicted by anisotropic yield stress.

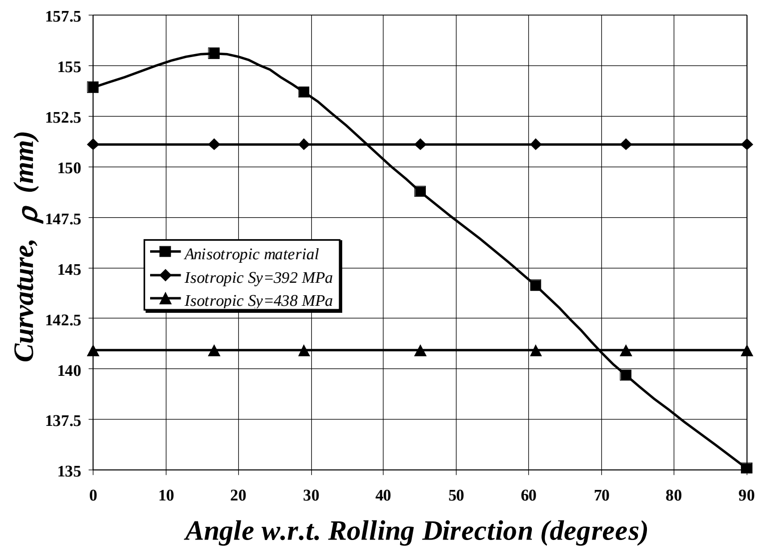

Figure 8. Variation of ρ to the angle w.r.t. the rolling direction.

Figure 8 shows a trend similar to the Figure 6 (big radius of curvature means small springback). The trend of the radius of curvature presented in Figure 8 agrees with investigations reported previously, it increases with the inverse of the yield stress. Again the springback predicted by the isotropic yield criteria does not agree with the anisotropic one and, the maximum SB (minimum radius) occur when the strip is cut along the transversal direction of the sheet.

The magnitude of the angle of twist (θ_3) was very small (0.03-0.05 degrees) and this may be attributed to computer-numerical rounding.

CONCLUSIONS

For anisotropic materials, springback depends on the angle of orientetion to the principal directions to the rolling sheet.

Springback obtaining from anisotropic sheet can exceed the springback bounds predicted with isotropic materials of similar properties.

In order to reduce the amount of springback in an application similar to that studied in this paper, the strip has to be cut along the rolling direction.

ACKNOWLEDGMENT

The authors would like to thank the U.S. Steel Technical Center in Monroville, PA, for providing the technical data, assistance and financial support. The Web Mechanics Group at the University of Pittsburgh was instrumental in initialing this research project.

REFERENCES

ANSYS (September 1998). “ANSYS/LS-DYNA (version. 5.6) Theoretical Manual.”

BARLAT, F. and LIAN, J. (1989). “Plastic Behavior and Stretchability of Sheet Metals. Part I: A Yield Function for Orthotropic Sheets Under Plane Stress Conditions,” International Journal of Plasticity, Vol. 5, pp.51-66.

BARLAT, F. (1987). “Crystallographic Texture, Anisotropic Yield Surfaces and Forming Limits of Sheet Metals,” Journal of Material Science and Engineering, 91, pp 55-72.

BARLAT, F. and RICHMOND, O. (1987). “Prediction of Tricomponent Plane Stress Yield Surfaces and Associated Flow and Failure Behavior of Strongly Textured F.C.C. Polycrystalline Sheets,” Journal of Material Science and Engineering, 95, pp 15-29.

DIETER, G. E. (1986). “Mechanical Metallurgy,” 3rd ed., Mc Graw-Hill, New York.

DU, C., ZHANG, L. and WANG, N., “Springback Prediction in Sheet Forming Simulation,” SAE technical paper series n^{o} 940937, Vol. 103, section 5, pp.707-717.

HALLQUIST, J. (May 1998). “LS-DYNA (version 950) Theoretical Manual,” Livemore Software Technology Corporation.

HILL, R. (1960). “The Mathematical Theory of Plasticity,” University Press, pp 317-340.

MAKER, B. (1998). “Implicit Springback Calculation using LS-DYNA,” Proceeding of the 5th International LS-DYNA Users Conference, Michigan, September 21-22.

MING, S. and LI, Z. (1999). “Issues Concerning Material Constitutive Laws and Parameters in Springback Simulations,” SAE Special Publication, SP-1435, pp.107-114. Paper n^{o} 1999-01-10002.

SHI, M. F., PRINCE, D. G. and SONG, W. (1998). “A Sensitivity Study of Simulation Parameters in Sheet Metal Forming and Springback Simulation using LS-DYNA,” Proceeding of the 5th International LS-DYNA Users Conference, Michigan, September 21-22.

STEIN, J. J. (1998). “The Effect of Process Variables on Sheet Metal Springback,” SAE technical paper series n^{o} 982299, 1998. Reprinted from: Proceeding of the International Body Conference and Exposition, Detroit, September 29 to October 1, p. 334.

YANG, H. (1999). “A Few Issues On Accuracy of Springback Simulation of Automobile Parts,” SAE Special Publication, SP-1435, pp. 101-105, SAE Paper n^{o} 1999-01-1000.

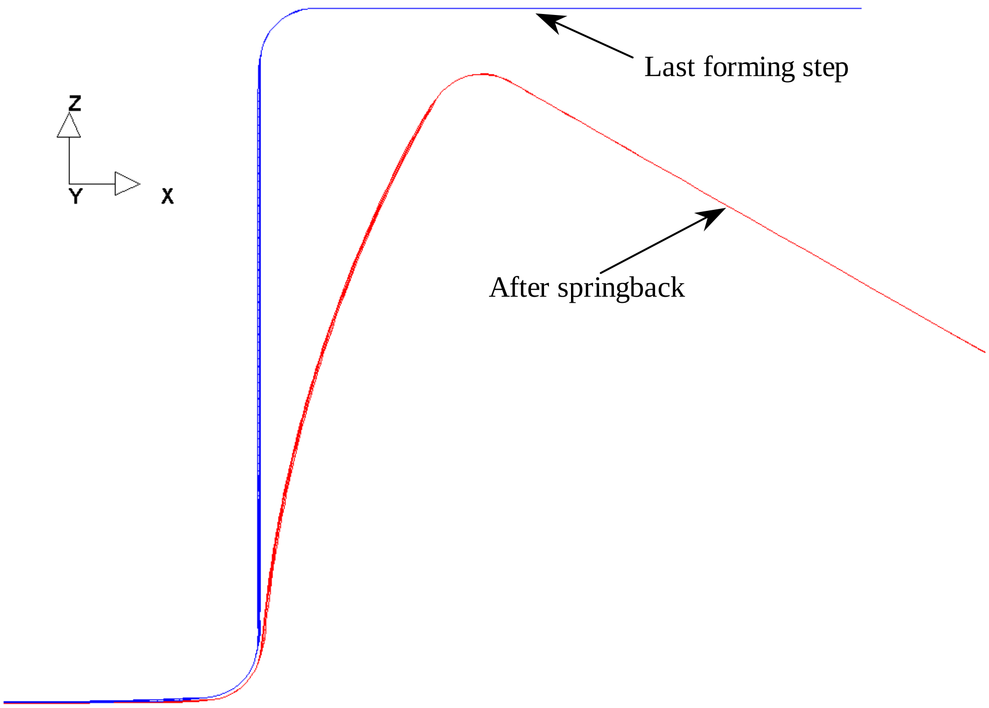

Figure 9. Change in shape after the last forming step due to springback (front view).

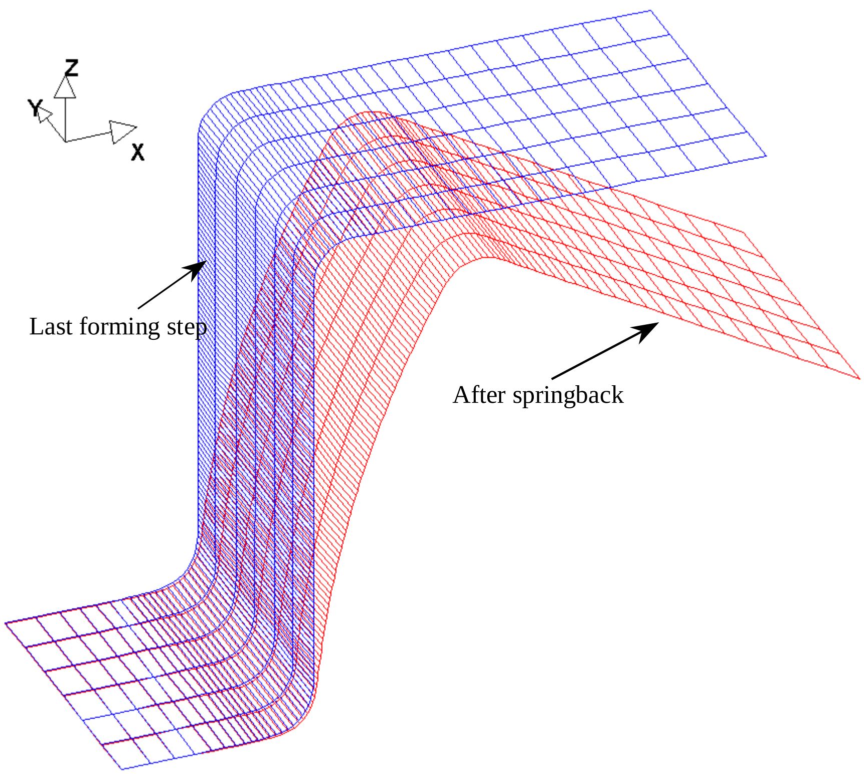

Figure 30. Change in shape after last forming step due to springback (isometric of view).